2008 IEEE/RSJ International Conference on Intelligent Robots and Systems
Acropolis Convention Center
Nice, France, Sept, 22-26, 2008

Parametric Excitation Based Gait Generation for Ornithoid Walking

Yuji Harata, Fumihiko Asano, Kouichi Taji and Yoji Uno

Abstract— **The parametric excitation based gait generation method proposed by Asano et al. restores mechanical energy lost by heel-strike collisions. Harata et. al. applied this method to a kneed biped robot which is proper for the parametric excitation, and show that sustainable gait has been generated with only knee torque. A swing-leg of a kneed biped robot has similar mechanism to an acrobot, and many acrobots bends a joint in inverse direction like ornithoid walking. This suggests that inverse bending a knee restores more mechanical energy than forward bending like human walking, and hence, inverse bending may be more efficient. In this paper, we propose a parametric excitation based ornithoid gait generation method for a kneed biped robot, and show that it can walk sustainably by numerical simulation. We also show that parametric excitation based inverse bending walking is more efficient than parametric excitation based forward bending walking with respect to performance indices in our model.**

I. INTRODUCTION

When a biped robot walks, collision occurs at the ground and hence, mechanical energy is lost. Therefore restoration of mechanical energy is requisite for sustainable walking of biped. In passive dynamic walking proposed by McGeer [1], potential energy is transported to kinetic energy as walking down a slope. For sustainable walking on a level ground, several methods for restoration of mechanical energy lost by the collisions were proposed.

Asano et al. [2] proposed a so-called virtual passive dynamic walking in which the virtual gravity was adequately designed by ankle and hip torque so as to restore kinetic energy lost by collision. Goswami et al. [3] proposed energy tracking control that the ankle and hip torque were designed to make energy constant during the sustainable gait and showed that the energy tracking control made stable limit cycle.

Another approach to restore mechanical energy is based on parametric excitation. A children's swing is an example of parametric excitation. When playing on the swing, a person is to bend and stretch to increase amplitude of vibration. In other words, without applying external force in direction of movement, up-and-down motion increases total mechanical energy. Fig. 1 presents the optimal trajectory, A→B→C→D→E, given by Lavrovskii and Formalskii [4], along which the increase of total mechanical energy is maximized, supposed that the length of a pendulum, l, is changed instantaneously. However, the length can not be actually changed instantaneously, and hence, in most practical situations a reference trajectory close to the optimal trajectory is chosen to restore total mechanical energy. Asano et al. [5] applied parametric excitation principle to a biped robot with telescopic legs which make the swing-leg mass up-and-down, and showed that the robot sustainably walked. Hayashi et. al. [6] applied parametric excitation to a real machine.

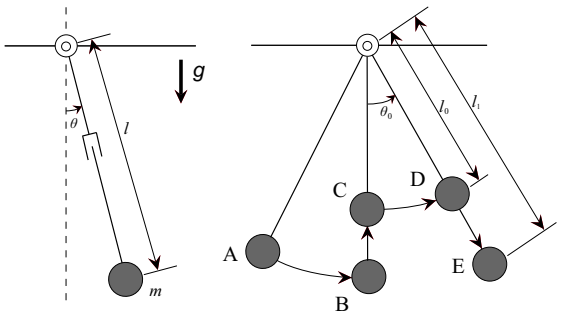

Fig. 1. Optimal trajectory of pendulum for parametric excitation

The telescopic leg has another advantage that up-and-down motion of swing-leg avoids scuffing the ground. Therefore, this method resolves both the energy restoration and foot clearance simultaneously. Harata et. al. [7] applied the parametric excitation principle to a kneed biped robot. Bending and stretching a swing-leg knee has the same effect of up-and-down of the center of mass of swing-leg. Like telescopic leg, mechanical energy was shown to restore by only bending and stretching a knee without hip actuation.

Swing-leg with an actuated knee has similar mechanism to an acrobot [8]. An acrobot can be controlled to swing up and balance about vertical equilibrium. This swing up motion needs to increase mechanical energy. The acrobot bends in inverse direction in a similar fashion of giant swing on a horizontal bar. This suggests that inverse bending knee like ornithoid shown in Fig. 2 restores more mechanical energy than forward bending like human walking. We note that, regardless of bending direction, the center of mass of swing-leg move up-and-down and mechanical energy can be restored.

In this paper, we propose and study parametric excitation based ornithoid walking. First, we propose parametric excitation based gait generation method for ornithoid walking and show that the robot can walk sustainably. Then, we compare inverse bending with forward bending for our biped model, and show that inverse bending parametric excited walking is more efficient than forward bending with respect

Y. Harata, K. Taji and Y. Uno are with the Department of Mechanical Science and Engineering, Graduate School of Engineering, Nagoya University, Furocho, Chikusa, Nagoya, 464-8603, Japan {y_harata, taji, uno}@nuem.nagoya-u.ac.jp

F. Asano is with the BMC RIKEN, 2271-130, Anagahora, Shimoshidami, Moriyama-ku Nagoya, 463-0003 Japan asano@bmc.riken.jp

Fig. 2. Ornithoid walking

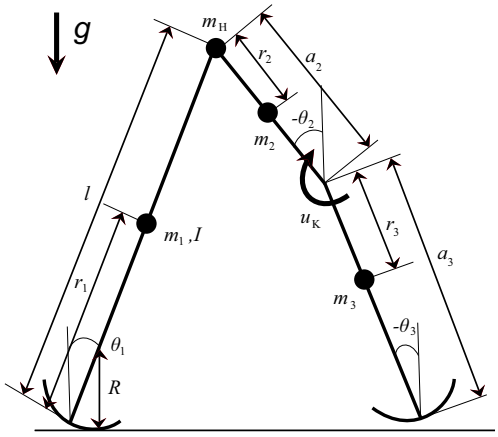

Fig. 3. Model of planar kneed biped robot with semi-circular feet

to performance indices such as walking speed and specific resistance.

This paper is organized as follows: Section II explains the biped robot with semicircular feet. Section III is the main part of this paper, in which we propose a sustainable gait generation method for ornithoid walking (Section III-B). We also compare parametric excitation based inverse bending walking to forward bending walking with our biped model (Section IV). Finally in Section V, we conclude this paper.

II. MODEL OF PLANAR KNEED BIPED ROBOT WITH SEMICIRCULAR FEET

Fig. 3 illustrates a biped robot discussed in this paper. The robot has four point mass and three degrees of freedom, and has semicircular feet whose centers are on each leg. Since there are two mass on the leg, the support-leg has inertia moment. The dynamic equation during single support phase takes the form

$$\boldsymbol{M}(\boldsymbol{\theta})\ddot{\boldsymbol{\theta}} + \boldsymbol{C}(\boldsymbol{\theta}, \dot{\boldsymbol{\theta}})\dot{\boldsymbol{\theta}} + \boldsymbol{g}(\boldsymbol{\theta}) = \boldsymbol{S}u_K - \boldsymbol{J}^{\mathrm{T}}\lambda, \qquad (1)$$

where $\boldsymbol{\theta} = [\ \theta_1 \quad \theta_2 \quad \theta_3\ ]^{\mathrm{T}}$ is the generalized coordinate vector, $\boldsymbol{M}$ is the inertia matrix, $\boldsymbol{C}$ is the Coriolis force and the centrifugal force, and $\boldsymbol{g}$ is the gravity vector. The matrix $\boldsymbol{J} = [\ 0 \quad 1 \quad -1\ ]$ is a Jacobian derived from a knee constraint, $\theta_2 = \theta_3$, and $\lambda \in \mathbb{R}$ is knee binding force. The control input vector, $\boldsymbol{S}u_K$, is described in detail later (Section III). In this robot, collisions occur at a knee and ground. The robot gait consists of the following three phases.

- The first phase (Single support phase I): The support-leg rotates around the contact point between a semicircular foot and ground, and the knee of swing-leg is not fixed, that is, knee binding force λ equals to zero, and hence, the knee of swing-leg can be bent by input torque.
- The second phase (Single support phase II): The support-leg rotates around the contact point and the knee of swing-leg is locked in a straight posture by knee binding force. When the first phase changes to the second phase, a completely inelastic collision is assumed to occur at a knee.
- The third phase (Double support phase): This phase occurs instantaneously, and the support-leg and the swing-leg are exchanged after the collision at the ground.

We first explain the impact equation at a knee of swing-leg. Let the coordinates $\dot{\boldsymbol{\theta}}^-$ and $\dot{\boldsymbol{\theta}}^+$ correspond to before and after knee collision, respectively. Then these are related by the equation

$$\boldsymbol{M}\dot{\boldsymbol{\theta}}^+ = \boldsymbol{M}\dot{\boldsymbol{\theta}}^- + \boldsymbol{J}^{\mathrm{T}}\lambda_K, \qquad (2)$$

where λ_K is constraint force making $\boldsymbol{J}\dot{\boldsymbol{\theta}}^+ = 0$. This force is given by

$$\lambda_K = -(\boldsymbol{J}\boldsymbol{M}^{-1}\boldsymbol{J}^{\mathrm{T}})^{-1}\boldsymbol{J}\dot{\boldsymbol{\theta}}^- \qquad (3)$$

From Eqs. (2) and (3), angular velocities after knee collision are given by

$$\dot{\boldsymbol{\theta}}^+ = (\boldsymbol{I} - \boldsymbol{M}^{-1}\boldsymbol{J}^{\mathrm{T}}(\boldsymbol{J}\boldsymbol{M}^{-1}\boldsymbol{J}^{\mathrm{T}})^{-1}\boldsymbol{J})\dot{\boldsymbol{\theta}}^-. \qquad (4)$$

We also assume that, once after knee collision, a knee-joint is fixed by the force $\boldsymbol{J}^{\mathrm{T}}\lambda$ until collision at the ground.

Next, we explain the impact equation at the ground. We assume also that a collision at the ground is completely inelastic. Generalized coordinate legs $i, (i = 1, 2)$ for separated

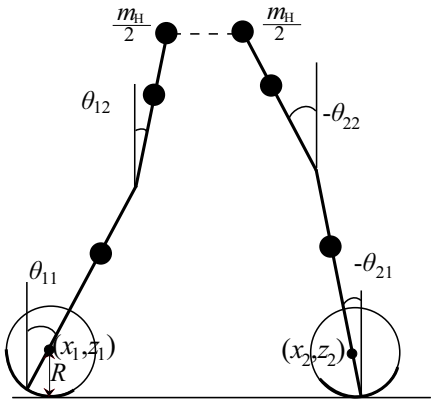

Fig. 4. Geometric relation at the heel-strike instant

model shown by Fig. 4 is given by

$$\boldsymbol{q} = \begin{bmatrix} \boldsymbol{q}_1 \\ \boldsymbol{q}_2 \end{bmatrix}, \tag{5}$$

where $\boldsymbol{q}_i = \begin{bmatrix} x_i & z_i & \theta_{i1} & \theta_{i2} \end{bmatrix}^{\mathrm{T}}$. Let "$-$" and "$+$" be superscripts corresponding to before and after impact at the ground, respectively. Then, we have $\boldsymbol{q}^+ = \boldsymbol{q}^-$, because the positions do not change before and after the impact. The impact equation of generalized coordinates takes the form

$$\bar{\boldsymbol{M}}(\boldsymbol{q})\dot{\boldsymbol{q}}^+ = \bar{\boldsymbol{M}}(\boldsymbol{q})\dot{\boldsymbol{q}}^- - \boldsymbol{J}_I(\boldsymbol{q})^{\mathrm{T}}\boldsymbol{\lambda}_I, \tag{6}$$

where $\boldsymbol{\lambda}_I \in \mathbb{R}^6$ is undetermined multiplier vector corresponding to impulse force and $\boldsymbol{J}_I \in \mathbb{R}^{6\times 8}$ is the Jacobian such that

$$\boldsymbol{J}_I(\boldsymbol{q})\dot{\boldsymbol{q}}^+ = \boldsymbol{0}_{6\times 1}. \tag{7}$$

There are some constraints among the coordinates. From geometric conditions, we have

$$\begin{aligned} &z_2 = R, \\ &x_1 + (a_3 - R)\sin\theta_{11} + a_2\sin\theta_{12} \\ &\quad = x_2 + (a_3 - R)\sin\theta_{21} + a_2\sin\theta_{22}, \\ &z_1 + (a_1 - R)\cos\theta_{11} + a_2\cos\theta_{12} \\ &\quad = z_2 + (a_1 - R)\cos\theta_{21} + a_2\cos\theta_{22}. \end{aligned} \tag{8}$$

These equations mean that the height of the center of foot of support-leg is constant (equal to foot radius) and that hip position (vertical and horizontal) from (x_1, z_1) equals to hip position from (x_2, z_2). In addition, the rate constraint that a foot of support-leg rolls on the ground is given by

$$\dot{x}_2^+ = R\dot{\theta}_{21}^+. \tag{9}$$

The rate constraints that knees are fixed in a straight posture are given by

$$\begin{aligned} \dot{\theta}_{11}^+ &= \dot{\theta}_{12}^+, \\ \dot{\theta}_{21}^+ &= \dot{\theta}_{22}^+. \end{aligned} \tag{10}$$

The Jacobian $\boldsymbol{J}_I$ is derived by differentiating Eq. (8) and by incorporating Eqs. (9) and (10).

The multiplier vector $\boldsymbol{\lambda}_I$ is given by

$$\boldsymbol{\lambda}_I = \boldsymbol{X}_I^{-1}\boldsymbol{J}_I\dot{\boldsymbol{q}}^-, \tag{11}$$

where matrix $\boldsymbol{X}_I$ is

$$\boldsymbol{X}_I = \boldsymbol{J}_I\bar{\boldsymbol{M}}^{-1}\boldsymbol{J}_I^{\mathrm{T}}. \tag{12}$$

Therefore the velocity of generalized coordinate after collision becomes

$$\dot{\boldsymbol{q}}^+ = (\boldsymbol{I}_8 - \bar{\boldsymbol{M}}^{-1}\boldsymbol{J}_I^{\mathrm{T}}\boldsymbol{X}_I^{-1}\boldsymbol{J}_I)\dot{\boldsymbol{q}}^-. \tag{13}$$

The semicircular feet have been shown to have same effects of equivalent ankle torque and to decrease energy dissipation of the collision at the ground [9]. Note again that only knees are actuated in our model.

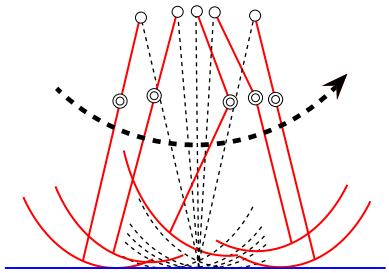

(a) Forward bending

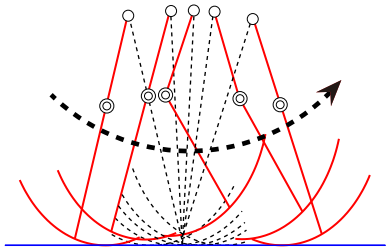

(b) Inverse bending

Fig. 5. Forward bending and inverse bending

III. ORNITHOID GAIT GENERATION

When parametric excitation principle applied to a kneed biped robot, the center of mass of swing-leg moves up-and-down by bending and stretching a knee. We remark that this motion occurs regardless of bending direction, i.e., inverse bending like ornithoid has the same effect of moving the center of mass as forward bending like human walking. Thus it is expected that a sustainable gait based on parametric excitation also can be invoked by inverse bending a knee. In the rest of paper, we call a knee bending like Fig. 5(a) forward bending and that like Fig. 5(b) inverse bending.

When the acrobot is control to swing up, energy restoration is necessary. The many acrobots are bent in inverse direction when swinging up. This suggests that the inverse bending a knee can increase more mechanical energy than the forward bending.

A. Control input design

In this section, we explain control design for a kneed biped robot shown by Fig. 3.

We first explain a reference trajectory. We give the refer-

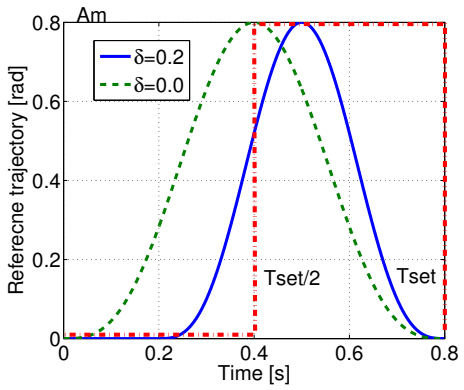

Fig. 6. Reference trajectory

ence trajectory for the relative knee-joint angle as

$$(\theta_2-\theta_3)_d = f(t) = \begin{cases} \alpha A_m \sin^3\left(\frac{\pi}{T_{\rm set}-\delta}(t-\delta)\right) & (\delta \le t \le T_{\rm set}) \\ 0 & (\text{otherwise}), \end{cases} \tag{14}$$

where $\delta > 0$ is bending delay A_m, is desired amplitude of vibration and $T_{\rm set}$ is the desired settling-time which is the period during bending and stretching a knee. The parameter $\alpha = \pm 1$ is used to indicate bending direction, that is, $\alpha = 1$ indicates inverse bending and $\alpha = -1$ indicates forward bending. Here, we choose the instance just after the third phase as the initial time of cycle, $t = 0$. The reason why introducing bending delay δ is illustrated by Fig. 6. In Fig. 6, a (red) dashed-dotted line is optimal trajectory for parametric excitation shown in Fig. 1, a (green) dot-line is the case of $\delta = 0$ [s] and a (blue) solid line is the case of $\delta = 0.2$ [s]. It is shown in Fig. 6 by introducing bending delay δ that the reference trajectory ((blue) solid line) approaches the optimal trajectory, and hence, it is expected to restore more mechanical energy than those without delay.

In the following, we design control input to track the reference trajectory given by Eq. (14). Let define $\boldsymbol{x} = \left[\begin{array}{ccc} \theta_1 & \theta_2 & \theta_2-\theta_3-f \end{array}\right]^{\rm T}$, and let $\boldsymbol{\theta}$ be rewritten by

$$\boldsymbol{\theta} = \begin{bmatrix} 1 & 0 & 0 \\ 0 & 1 & 0 \\ 0 & 1 & -1 \end{bmatrix} \boldsymbol{x} + \begin{bmatrix} 0 \\ 0 \\ -f \end{bmatrix} =: \boldsymbol{L}\boldsymbol{x} + \boldsymbol{N}. \tag{15}$$

Then $\dot{\boldsymbol{\theta}}$ and $\ddot{\boldsymbol{\theta}}$ are

$$\dot{\boldsymbol{\theta}} = \boldsymbol{L}\dot{\boldsymbol{x}} + \dot{\boldsymbol{N}}, \tag{16}$$

$$\ddot{\boldsymbol{\theta}} = \boldsymbol{L}\ddot{\boldsymbol{x}} + \ddot{\boldsymbol{N}}. \tag{17}$$

The dynamic equation (1) in the first phase is redefined as

$$\boldsymbol{M}\boldsymbol{L}\ddot{\boldsymbol{x}} + \boldsymbol{M}\ddot{\boldsymbol{N}} + \boldsymbol{C}\boldsymbol{L}\dot{\boldsymbol{x}} + \boldsymbol{C}\dot{\boldsymbol{N}} + \boldsymbol{g} = \boldsymbol{S}u_K. \tag{18}$$

Since the proposed robot has only knee actuation (Fig. 3), the control input vector is given by

$$\boldsymbol{S} = \begin{bmatrix} 0 \\ -1 \\ 1 \end{bmatrix}. \tag{19}$$

TABLE I

PHYSICAL PARAMETERS OF THE KNEED BIPED ROBOT

r_1	0.40	m	R	0.575	m
r_2	0.20	m	m_1	5.0	kg
r_3	0.30	m	m_2	1.0	kg
a_2	0.40	m	m_3	4.0	kg
a_3	0.60	m	m_H	5.5	kg
l	1.0	m	I	2.0	kgm^2

Let define K as

$$K = \left[\begin{array}{ccc} 0 & 0 & 1 \end{array}\right] \boldsymbol{L}^{-1}\left[\boldsymbol{M}^{-1}\boldsymbol{S}\right], \tag{20}$$

and select the knee torque u_K as

$$u_K = K^{-1}Z, \tag{21}$$

where Z is defined by

$$Z = \left[\begin{array}{ccc} 0 & 0 & 1 \end{array}\right] \boldsymbol{L}^{-1}\boldsymbol{M}^{-1}(\boldsymbol{M}\ddot{\boldsymbol{N}} + \boldsymbol{C}\boldsymbol{L}\dot{x} + \boldsymbol{C}\dot{\boldsymbol{N}} + \boldsymbol{g}). \tag{22}$$

Using Eqs. (19)–(22), the dynamic equation (18) reduces to

$$\ddot{\theta}_2 - \ddot{\theta}_3 = \ddot{f}. \tag{23}$$

By integrating this equation twice, we obtain

$$\begin{aligned} &(\theta_2(t)-\theta_3(t)) - (\theta_2(0)-\theta_3(0)) - (\dot{\theta}_2(0)-\dot{\theta}_3(0))t \\ &= f(t) - f(0) - \dot{f}(0)t. \end{aligned} \tag{24}$$

If initial states are set to equal initial states of the reference trajectory, i.e. $\dot{\theta}_2(0) - \dot{\theta}_3(0) = \dot{f}(0)$ and $\theta_2(0) - \theta_3(0) = f(0)$, then Eq. (24) can be rewritten as

$$\theta_2(t) - \theta_3(t) = f(t). \tag{25}$$

Therefore, the input u_K given by Eq. (21) is shown to track the reference trajectory $\theta_2 - \theta_3$.

B. Numerical simulation

We show simulation results of parametric excitation based ornithoid gait generation applied for a biped model (Fig. 3), whose parameters are shown by Table I. We note that in this model the shin mass is much larger (4 times) than the thigh mass unlike both human and bird. This is because energy restoration based on the parametric excitation principle needs up-and-down motion of the center of mass of swing-leg, i.e., if shin mass is small, knee bending make little up-and-down motion effect of the center of mass of swing-leg and hence, mechanical energy does not sufficiently restored.

In our simulation, the control input u_K defined by Eq. (21) is determined for the reference trajectory Eq. (14) with an amplitude $A_m = 0.8$ [rad], settling time $T_{set} = 0.8$ [s] and bending delay $\delta = 0.2$ [s]. For these parameters, the robot succeeds in walking sustainably.

Fig. 7 illustrates simulation results between 105 [s] and 108 [s] after the start of simulation in which the initial conditions are $[\boldsymbol{\theta}\ \dot{\boldsymbol{\theta}}] = [-0.21, 0.21, 0.21, 1.0, 0.90615, 0.90615]$. Fig. 7(a) shows angular positions, (b) shows angular velocities, (c) shows the total mechanical energy, (d) shows knee torque, u_K and (e) shows foot clearance. Foot clearance is

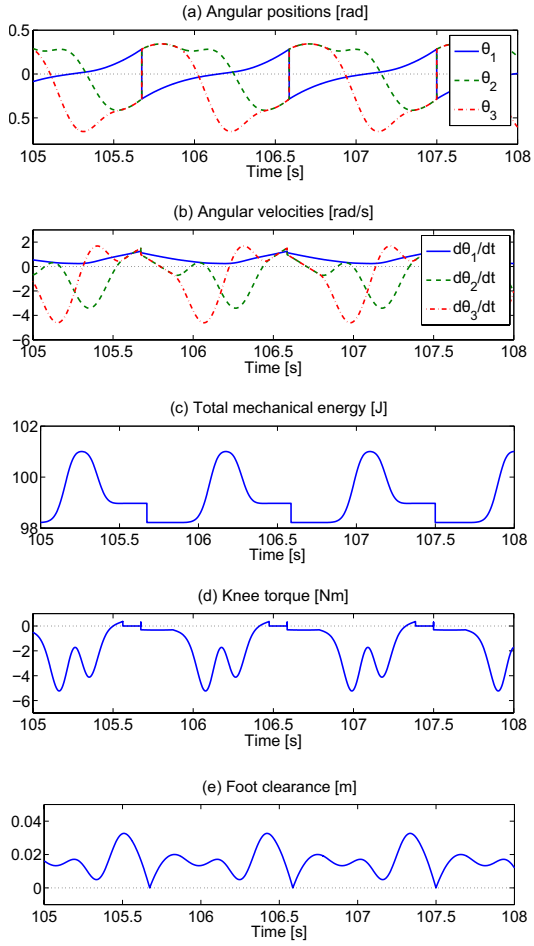

Fig. 7. Simulation results

the height of the bottom of swing-leg from the ground level. From Fig. 7(a), $\theta_2 - \theta_3$ is found to be always larger than or equal to 0, that is, knee is bent in inverse direction. From Fig. 7(c), energy dissipation of the collision at the knee is hardly observed, while energy dissipation of the collision at the ground is relatively large. Almost negligible energy is lost at the knee collision because the relative knee-joint angular velocity is very close to zero just before knee impact, according to the reference trajectory defined in Eq. (14). Fig. 7(e) shows that foot clearance is positive except for the third phase (double support phase), and hence, the biped avoids scuffing the ground. In summary, the figures show that the robot walks stably and sustainably with inverse bending. Fig. 8 shows stick diagram of one step for stable gait and this figure shows that a biped robot walks like ornithoid walking.

IV. COMPARISON BETWEEN INVERSE BENDING AND FORWARD BENDING FOR PARAMETRIC EXCITATION

We compare inverse bending walking to forward bending with respect to performance indices such as walking speed

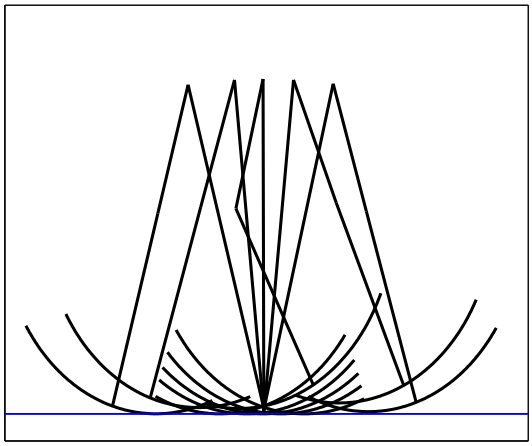

Fig. 8. Stick diagram of simulation results

and specific resistance. Specific resistance is defined by

$$\mu = \frac{\int_{0^+}^{T^-} |u_K(\dot{\theta}_2 - \dot{\theta}_3)|\mathrm{d}t/T}{M_g g \overline{V}/T}, \tag{26}$$

and represents energy efficiency. The smaller a specific resistance value is, the more efficient a walking is. In Eq. (26), 0^+ and T^- represent the time just after and before collision at the ground, respectively, M_g is the total mass of a biped robot and $\overline{V}$ is the average walking speed.

Comparison is performed by numerical simulation. In this simulation, a biped model and its physical parameters are the same as in the previous section. We research the influence of change of amplitude A_m on walking performance. We remark that an optimal bending delay δ is different between inverse bending and forward bending from the energy efficient view point. Therefore, we search optimal bending delays which minimize specific resistance of stable walking. In the simulation, we fix $T_{set} = 0.8$ [s] and the amplitude is changed from 0.6 [rad] to 1.3 [rad] by 0.02 [rad], and for each amplitude, we compare specific resistance for each delays from 0.1 [s] to 0.5 [s] by 0.02 [s]. With these optimal bending delays, we compare inverse bending walking with forward bending with respect to walking performance.

The results are shown in Fig. 9. (Blue) circles illustrate the results of inverse bending and (green) squares illustrate those of forward bending. Fig. 9 shows the simulation result; (a) optimal bending delay, (b) walking speed and (c) the specific resistance. We plot the value for which a biped robot can walk sustainably. Therefore, in the forward bending the results are plotted only larger than or equal to $A_m = 0.78$ [rad], while in the inverse bending the whole results are plotted. It is observed in Fig. 9(a) that the optimal bending delays of inverse bending are smaller than those of forward bending and the larger amplitude is, the smaller optimal bending delay is. It is observed in Fig. 9(b) that walking speed of

inverse bending is larger than those of forward bending, and the larger amplitude is, the larger the walking speed is. Fig. 9(c) shows that specific resistance of inverse bending is smaller than that of forward bending. We can observe from Fig. 9 that bifurcation occurs in inverse bending, when amplitude becomes larger than about 0.9 [rad]. From Fig. 9(a), an optimal bending delay obtained by our simulation is stepwise. This suggests that true optimal delay have not been obtained, because of coarse search step size. This may be a reason of bifurcations.

V. CONCLUSION

We have proposed an ornithoid gait generation method based on the parametric excitation for a biped robot, and showed by numerical simulation that the robot could walk sustainably. Numerical simulation also showed that the parametric excitation based inverse bending walking was more efficient than parametric excitation based forward bending walking with respect to the performance indices in our model. In the future work, we research the analytical optimal trajectory, for example, optimal bending delay.

VI. ACKNOWLEDGMENTS

This work was partly supported by JSPS Grant-in-Aid for Scientific Research (B) 18360202 and (C) 18560429.

REFERENCES

[1] T. McGeer: "Passive dynamic walking," Int. J. of Robotics Research, vol. 9, no. 2, pp.62-82, 1990.
[2] F. Asano, M. Yamakita and K. Furuta, "Virtual passive dynamic walking and energy-based control laws," *IEEE/RSJ Int. Conf. on Intelligent Robotics and Systems*, pp 1149-1154, 2000.
[3] A. Goswami, B. Espiau and A. Keramane, "Limit cycles in a passive compass gait biped and passivity-mimicking control laws," *J. of Autonomous Robots*, vol. 4, no. 3, pp 273-286, 1997.
[4] E.K. Lavrovskii and A.M. Formalskii, "Optimal control of the pumping and damping of swing," *J. of Applied Mathematics and Mechanics*, vol. 57, no. 2, pp 311-320, 1993.
[5] F. Asano, Z.W. Luo and S. Hyon, "Parametric excitation mechanisms for dynamic bipedal walking," *IEEE Int. Conf. on Robotics and Automation*, pp 611-617, 2005.
[6] T. Hayashi, F. Asano, Z.W. Luo, S. Hirano, A. Kato, "Parametric excitation approaches to efficient bipedal walking," Proceedings of the 2007 IEEE/RSJ International Conference on Intelligent Robots and Systems, pp 2210-2216, 2007.
[7] Y. Harata, F. Asano, Z.W. Luo, K. Taji, Y. Uno, "Biped gait generation based on parametric excitation by knee-joint actuation," Proceedings of the 2007 IEEE/RSJ International Conference on Intelligent Robots and Systems, pp 2198-2203, 2007.
[8] M. Spong, "The swing up control for the acrobot," *IEEE Control System Magazine*, vol. 15, no. 2, pp 49-55, 1995.
[9] F. Asano and Z.W. Luo, "The effect of semicircular feet on energy dissipation by heel-strike in dynamic bipedal locomotion," *IEEE Int. Conf. on Robotics and Automation*, pp 3976-3981 2007.

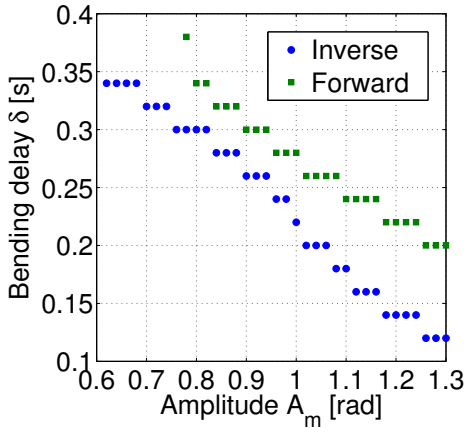

(a) Bending delay

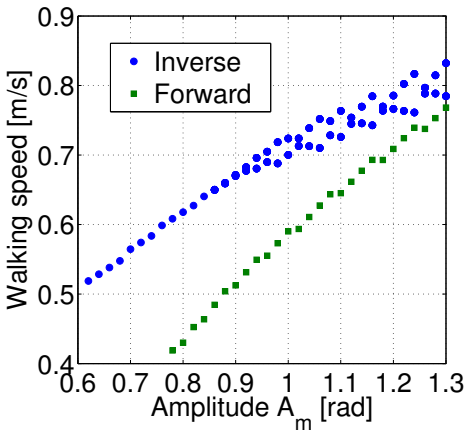

(b) Walking speed

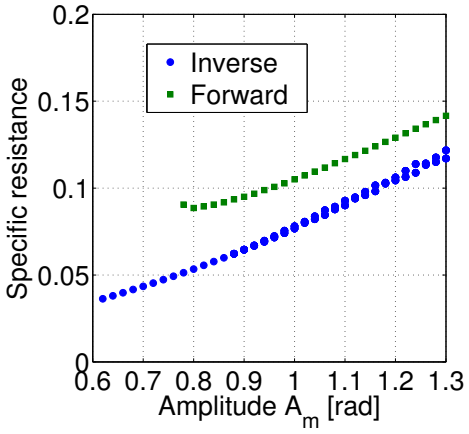

(c) Specific resistance

Fig. 9. Walking performance with respect to A_m